# THE IONIZED GAS AROUND STARFORMING GALAXIES

E.O. Vasiliev[1], M.V. Ryabova[2], Yu.A. Shchekinov[2]

[1]Institute of Physics, Southern Federal University, Stachki Ave. 194, Rostov-on-Don, 344090 Russia, *eugstar@mail.ru*

[2]Department of Physics, Southern Federal University, Sorge 5, Rostov-on-Don, 344090 Russia

ABSTRACT. We consider the evolution of metal-enriched gas exposed to a superposition of time-dependent radiation field of a nearby starburt galaxy and nearly invariant (on timescales 100 Myr) extragalactic ionization background. We study the evolution of ionic species (particularly those commonly observed in galactic circumference) depending on the galactic mass and star formation rate, and derive conditions for the highly ionized oxygen, OVI, to appear in extended galactic haloes in absorption or emission spectra. We have found that the maximum OVI fraction can reach $\sim 0.4 - 0.6$ under the action of both ionizing radiation field, which is typical in haloes of starforming galaxies, and the extragalactic background, the fraction remains high in a wide temperature range. We have shown that the OVI fraction is high enough that *even* for $\sim 0.1 Z_\odot$ metallicity we can explain large OVI column densities ($\log[\mathrm{N(OVI)}, \mathrm{cm}^{-2}] \sim 14.5 - 15.3$) observed in the haloes of staforming galaxies by Tumlinson et al. (2011). Thus, the requirements to the sources of oxygen supply into the extended haloes become reasonably conservative.

**Key words**: galaxies: evolution – haloes – starburt – theory – diffuse radiation – intergalactic medium – quasars: general – absorption lines – physical data and processes: atomic processes

## 1. Introduction

Huge (up to 150 kpc) halos of ionized gas in star-forming galaxies contain a substantial mass of metals and gas (Tumlinson et al., 2011). OVI is a fragile ionic state in the sense that under standard assumptions of thermal ionization its fraction never exceeds $\sim 0.2$ and such a high value is reached only in a narrow temperature range (Gnat & Sternberg 2007). Then, conservative estimates of a typical circumgalactic gaseous mass force to assume solar metallicity for gas extending up to 150 kpc in the halos of star-forming galaxies.

Here we study the evolution of ionic composition of a gas in the halos of star-forming galaxies taking into account starformation history.

## 2. The model and initial conditions

Our model includes the following ingredients

• the ionization and thermal evolution of gas (in a lagrangian element): nonequilibrium (time-dependent) ionization kinetics for H, He, C, N, O, Ne, Mg, Si, Fe and self-consistent cooling and heating rates, in total 96 ordinary differential equations (see details in Vasiliev, 2011);

• the extragalactic spectrum: Haardt & Madau (2001) spectra for 49 redshifts;

• the UV galactic spectrum was calculated using the PEGASE code (Fioc & Rocca-Volmerange 1997);

• the X-ray galactic spectrum calculated using the "$L_X - SFR$" relation (Gilfanov et al., 2004);

• a power-law starformation rate (SFR): $SFR(t) = M_g^{p_1}/p_2$, where $M_g$ is the galactic gaseous mass and $p_1 = 2$;

• the galactic halo gas exposed to the cumulative galactic and extragalactic ionizing radiation, the galactic part of the spectrum being attenuated by the underlying neutral gas: $\tau_\nu = \sigma_\nu^{\mathrm{HI}} N_{\mathrm{HI}} + \sigma_\nu^{\mathrm{HeI}} N_{\mathrm{HeI}}$, where $N_{\mathrm{HI}} = 10^{20}$ cm$^{-2}$, $N_{\mathrm{HeI}} = 10^{19}$ cm$^{-2}$ are assumed.

## 3. The initial conditions

We consider a gas in outer halo of massive starforming galaxies with stellar mass several $\times 10^{10}$ $M_\odot$. So that these galaxies are similar to the Milky Way. According to the recent simulations of the Milky Way galactic halo the number density of a gas in the the Galactic halo is found to range within $\sim (0.5 - 2) \times 10^{-4}$ cm$^{-3}$ at distances $\sim 50 - 300$ kpc (Feldmann et al., 2013). The observational estimates of the circumgalactic gas density give $\sim (1 - 3) \times 10^{-4}$ cm$^{-3}$ at $r \sim 40 - 150$ kpc (e.g. Anderson & Bregman 2010). So that in our calculations we adopt $n = 10^{-4}$ cm$^{-3}$ for the number density of the circumgalactic gas.

We start our calculation at $z = 2$ (the lookback time is ∼10 Gyrs). At first, this timescale is about cooling time for hot gas with $T \sim 10^6$ K and $\sim (0.5 - 2) \times 10^{-4}$ cm$^{-3}$ (Feldmann et al., 2013). At second, the last major merging for the Milky Way type galaxies is thought to be earlier than $z \sim 2$ (Hammer et al., 2007).

The initial ionic composition and temperature are set to the ones corresponding to photoequilibrium in a gas exposed to the extragalactic Haardt & Madau spectrum at $z = 2$. This radiation background is sufficiently high to force such low density gas into photoequilibrium (Vasiliev 2011). But one should note that the time of calculation is long enough compared to the relaxation scale of the ionization and thermal evolution of a gas exposed to the time-dependent spectrum adopted here.

We study the evolution of a gas with metallicity ranged from $10^{-2}$ to 0.1 $Z_\odot$. Higher metallicity is expected to be overestimation, the lower limit is corresponded to the upper limit of the IGM metallicity at $z \sim 2 - 3$ (e.g., D'Odorico et al., 2010).

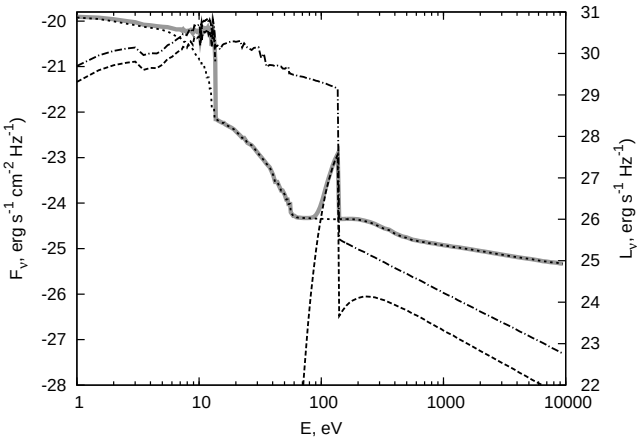


Figure 1: The cumulative ionizing background flux (thick grey line) at $z = 0.2$ and a distance from the galaxy $d = 100$ kpc, which consists of the UV and X-ray galactic spectrum, attenuated by galactic neutral gas (dash line), the extragalactic ionizing background (dotted line). The galactic spectral luminosity is shown by dash-dotted line (the right axis).

## 4. Results

From the chemical evolution models calculated using the PEGASE code we obtain the time-dependent SFR, stellar mass, metallicity of a gas and spectral luminosity. We assume the initial gaseous mass is $M_g^i = 10^{11}\ M_\odot$. Here we consider two models with different parameter $p_2$: $3 \times 10^4$ Myr $M_\odot^{-1}$ – model A, and $5 \times 10^3$ Myr $M_\odot^{-1}$ – model C. Gas in model C is almost coverted into stars up to $\sim 10$ Gyr, whereas the galaxy in model A still remains gas-rich one: only $\sim 10$ % of gaseous mass goes into stars. In model A the SFR (absolute) is nearly constant at $\sim 6\ M_\odot$/yr during first 200 Myr afterwards decreases down to $\sim 0.6\ M_\odot$/yr at 10 Gyr. The corresponding values of SFR in model C are about 7 times higher, but the timescale, where the rate is constant, is shorter, $\sim 50$ Myr. Thus, the rates in both models remain still high at $\sim 5 - 10$ Gyr (redshifts $z \sim 0.5 - 0$) to consider such galaxies as starforming ones (Schiminovich et al., 2007).

Figure 1 presents the galactic spectral luminosity at $t = 7.5$ Gyr (that corresponds the time elapsed from $z = 2$ to 0.2) is shown by dash-dotted line (the right axis). One can note a significant break at 91 Å, this value corresponds to the minimum wavelength in the spectrum obtained in the PEGASE code. This value is resonable because of the exponential decrease of number of such hard photons emitted by stellar population (see e.g. Rauch 2003). Figure 1 demostrates an example of the total spectral distribution: the cumulative ionizing background flux (thick grey line) at $z = 0.2$ and distance $d = 100$ kpc from the galaxy. The total spectrum consists of the galactic (dash line) and extragalactic (dotted line) ionizing backgrounds. The strong absorption of the galactic photons within energy range, $E \sim 13.6 - 90$ eV, in the galactic disk leads to the control of ionic composition by the extragalactic background. To estimate a significance of the absorption one can see the galactic spectral luminosity (see the right axis). Note that there is a bump around $E \sim 90 - 136$ eV, because not all photons emitted by galactic stellar population are absorbed in the disk. Certainly, this is due to our choice of the neutral column densities $N_{\rm HI}$ and $N_{\rm HeI}$ in the disk. In case of the higher column densities the amplitude of the bump decreases. Also the decrease is taken place at large distances from the galaxy, where the extragalactic radiation is dominant. Note that in the range $E \sim 90 - 136$ eV there is the OV ionization potential, $I_{\rm OV} = 113.9$ eV. So that the excess of such photons is expected to change the ionization kinetics of oxygen and may lead to higher OVI fraction.

Figure 2 shows the evolution of OVI fraction in a gas located at different distances from the galactic center. Because of high flux of ionizing radiation at $z \sim 2$ oxygen is mainly locked in the OVII state. The decrease of the ionizing flux with redshift or/and due to decrease of SFR leads to the OVII recombination and growth of the OVI fraction. Actually, after $\sim 1 - 2$ Gyr because the SFR goes down in $\sim 3 - 4$ times compared to the initial value, galactic luminosity decreases, so that the transition from OVII to OVI becomes faster. Under the standard conditions the OVI state is fragile and further recombination leads to lower ionic states. However, the excess of photons with $E > I_{\rm OV} = 113.9$ eV emitted by starforming galaxies does not allow to develop recom-

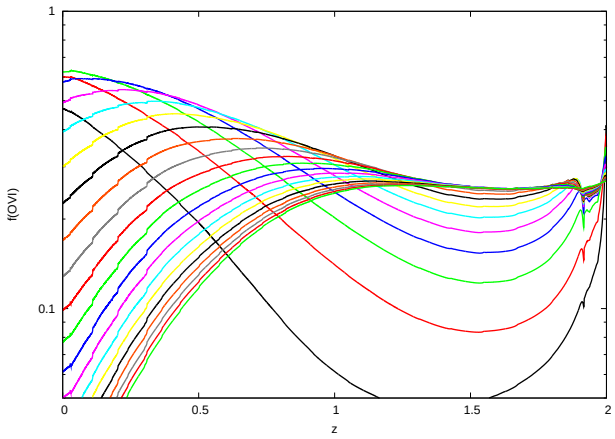


Figure 2: OVI fraction evolution of gas at different distances from the galactic center (the distances vary from 50 to 250 kpc with step 10 kpc from bottom line)

bination so efficiently: it is almost freezed out at OVI. In our models the OVI fraction reaches $\sim 0.4-0.6$ in a gas with metallicity 0.1 $Z_\odot$. This results in a factor of 2-3 more conservative estimate of the oxygen mass in haloes compared to $M_O = 1.2\times10^7(0.2/f_{OVI})\ M_\odot$ (Tumlinson et al., 2011). Thus, the OVI fraction is higher than that in the standard (photo-)equilibrium case, where the maximum OVI fraction is $\sim 0.1-0.2$ (e.g., Gnat & Sternberg 2007).

Figure 3 presents the dependence of the OVI column density on the impact parameter assuming 1/10 of solar metallicity gas exposed to the ionizing background evolved as in models A and C (small symbols near right axis, types of symbols correspond to different redshifts). For $0.1Z_\odot$ the OVI column density ranges in $\log[\mathrm{N(OVI)},\mathrm{cm}^{-2}] \sim 14.3-15.3$ at impact parameter $b < 150$ kpc, that exibits a good coincidence with the observational data obtained by Tumlinson et al., 2011). Higher OVI fraction obtained in our model leads to more conservative estimate of the oxygen mass in haloes, and consequently weaker constrains on the sources of oxygen.

## 5. Conclusions

With minimum assumptions we have found physical conditions (density, metallicity of gas, the spectrum shape) under which the OVI fraction can reach $\sim 0.6$.

Using the PEGASE code we have calculated chemical and spectro-photometric evolution of galaxies, and have chosen two of the models whose sSFR and stellar masses are close to the star-forming galaxies with large OVI column densities (Tumlinson et al., 2011).

We have found that OVI column densities range in $\log[\mathrm{N(OVI)},\mathrm{cm}^{-2}] \sim 14.5-15.3$ for $0.1Z_\odot$ gas, and $\sim 12.9-14.2$ for $0.01Z_\odot$ gas at impact parameters up to $<$ 150 kpc. This results in a factor of 2-3 more conservative estimate of the oxygen mass in halos compared to $M_O = 1.2\times10^7(0.2/f_{OVI})\ M_\odot$ (Tumlinson et al., 2011).

*Acknowledgements.* This work is supported by the RFBR through the grants 12-02-00365, 12-02-00917, 12-02-92704, and by the Ministry of education and science of Russian Federation (state contracts 14.A18.21.1304, 2.5641.2011, 14.18.21.1179). EV is grateful for support from the "Dynasty" foundation.

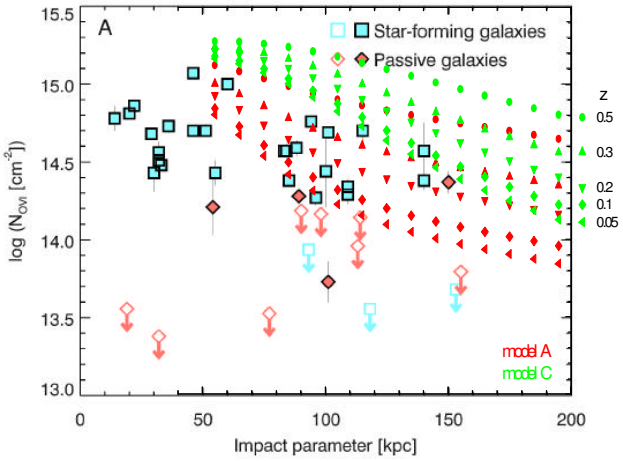


Figure 3: The dependence of the OVI column density on the impact parameter. The filled red and green symbols correspond to models A and C. Different type of symbols show the column densities for several redshift $z$ (depicted near the right axis). The metallicity of gas is 0.1 $Z_\odot$. The underlying picture is taken from the paper by Tumlinson et al. (2011).

## References

Anderson M.E., Bregman J.N.: 2010, *ApJ*, **714**, 320.
D'Odorico V., Calura F., Cristiani S., Viel M.: 2010, *MNRAS*, **401**, 2715.
Fioc M., Rocca-Volmerange B.: 1997, *A&A*, **326**, 950.
Gilfanov M., Grimm H.-J., Sunyaev R., 2004, *MNRAS*, **347**, L57.
Gnat O., Sternberg A.: 2007, *ApJS*, **168**, 213.
Haardt F., Madau P.: 2001, in *Clusters of Galaxies and the High Redshift Universe Observed in X-rays*, ed. D.M.Neumann & J.T.V.Tran
Hammer F., Puech M., Chemin L. et al.: 2007, *ApJ*, **662**, 322.
Rauch T.: 2003, *A&A*, **403**, 709.
Schiminovich D. et al.: 2007, *ApJSS*, **173**, 315.
Tumlinson J. et al.: 2011, *Science*, **334**, 948.
Vasiliev E.O.: 2011, *MNRAS*, **414**, 3145.